



# **Analysis of Thermal Boundary Layer Flow over a Vertical Plate with Electrical Conductivity and Convective Surface Boundary Conditions**

**O. J. Fenuga<sup>1\*</sup>, I. O. Abiala<sup>1</sup> and S. O. Salawu<sup>2</sup>**

<sup>1</sup>*Department of Mathematics, University of Lagos, Akoka, Lagos, Nigeria.*

<sup>2</sup>*Department of Mathematics, University of Ilorin, Ilorin, Nigeria.*

## **Authors' contributions**

*This work was carried out in collaboration between all authors. Author OJF designed the study, performed the numerical/statistical analysis, wrote the protocol and wrote the first draft of the manuscript. Author IOA managed the analysis of the study. Author SOS managed the literature searches. All authors read and approved the final manuscript.*

## **Article Information**

DOI: 10.9734/PSIJ/2018/37678

### Editor(s):

(1) Lei Zhang, Winston-Salem State University, North Carolina, USA.

(2) Roberto Oscar Aquilano, School of Exact Science, National University of Rosario (UNR), Rosario, Physics Institute (IFIR)(CONICET-UNR), Argentina.

### Reviewers:

(1) John Abraham, University of St. Thomas, USA.

(2) Jagdish Prakash, University of Botswana, Botswana.

(3) Venkateswarlu Malapati, V. R. Siddhartha Engineering College, India.

(4) Alok Kumar Pandey, Roorkee Institute of Technology, India.

Complete Peer review History: <http://www.sciedomain.org/review-history/23124>

**Original Research Article**

**Received 24<sup>th</sup> October 2017**  
**Accepted 6<sup>th</sup> December 2017**  
**Published 10<sup>th</sup> February 2018**

## **ABSTRACT**

This paper analyses the thermal boundary layer flow over a vertical plate with electrical conductivity and convective surface boundary conditions. Transforming the governing nonlinear partial differential equations into a set of coupled non-linear ordinary differential equations by using the usual similarity transformation, the resulting coupled nonlinear ordinary differential equations are solved numerically by Runge- Kutta fourth order method with shooting technique. The behaviour and properties of thermo physical parameters in the fluid flow on the structure of the velocity and temperature fields are presented graphically and discussed.

**Keywords:** *Electrical conductivity; thermal boundary layer; vertical plate; convective surface boundary conditions.*

\*Corresponding author: E-mail: ofenuga@unilag.edu.ng;

## 1. INTRODUCTION

The study of heat transfer is an integral part of natural convection flow and a class of boundary layer theory. The quantity of heat transferred is highly dependent on the fluid motion within the boundary layer.

Convective heat transfer studies are very important in processes involving high temperature such as gas turbines, nuclear plants, thermal energy storage, etc. The solution for the laminar boundary layer problem on a horizontal flat plate was obtained by Heinrich Blasius [1] and since then it has been a subject of current research. Aziz [2] investigated a similarity solution for laminar thermal boundary layer over a flat-plate with a convective surface boundary condition. Bataller [3] presented a numerical solution for the combined effects of thermal radiation and convective surface heat transfer on the laminar boundary layer about a flat-plate in a uniform stream of fluid (Blasius flow) and about a moving plate in a quiescent ambient fluid. Cortell [4] in his work presented a numerical solution of the Classical Blasius Flat-Plate Problem using a Runge-Kutta algorithm for higher order initial value problem. Cortell [5] investigated a similarity solution for flow and heat transfer of a quiescent fluid over a nonlinearly stretching surface. Gabriella [6] used an iterative transformation method for the solution of boundary layer problem of a non-Newtonian power law fluid flow along a moving plate surface. There was a drag coefficient dependent on the velocity ratio and on the power law exponent. He [7] worked on a simple perturbation approach to blasius equation. In his paper, he coupled the iteration method with the perturbation method to solve the well-known Blasius equation. Makinde and Olanrewaju [8] conducted a study on the effects of buoyancy force on thermal boundary layer over a vertical plate with convective surface boundary conditions. In Olanrewaju and etal [9], it was assumed that the lower surface of the plate is in contact with the hot fluid while a stream of cold fluid flows steadily over the upper surface with a heat source that decayed exponentially. Makinde [10] studied analysis of non-newtonian reactive flow in a cylindrical pipe. Makinde and Sibanda [11] conducted a study on magneto hydrodynamic mixed convective flow and heat and mass transfer past a vertical plate in a porous medium with constant wall suction. Shrama and Gurminder [12] looked at the effect of temperature dependent electrical conductivity

on steady natural convection flow of a viscous incompressible low Prandtl ( $Pr \ll 1$ ) electrically conducting fluid along an isothermal vertical non-conducting plate in the presence of transverse magnetic field and exponentially decaying heat generation. The study of an incompressible viscous and electrically conducting fluid in the presence of a uniform transverse magnetic field was investigated by Watunade and pop [13].

This paper is an extension of [8] with buoyancy force, convective surface boundary condition and electrical conductivity parameters. The numerical solutions of the resulting momentum and the thermal similarity equations are reported for representative values of thermo physical parameters characterizing the fluid convective process.

## 2. MATERIALS AND METHODS

Consider a two-dimensional steady incompressible fluid flow coupled with heat transfer by convection over a vertical plate. A stream of cold fluid at temperature  $T_\infty$  moving over the right surface of the plate with a uniform velocity  $U_\infty$  while the left surface of the plate is heated by convection from a hot fluid at temperature  $T_f$ , which provides a heat transfer coefficient  $h_f$  (see Fig. 1). The  $x$ -axis is taken along the plate and  $y$ -axis is normal to the plate. Magnetic field of intensity  $B_0$  is applied in the  $y$ -direction. It is assumed that the external field is zero. Incorporating the Boussinesq's approximation within the boundary layer, the governing equations of continuity, momentum and energy equations according to [8] are respectively given as:

$$\frac{\partial u}{\partial x} + \frac{\partial v}{\partial y} = 0 \quad (1)$$

$$u \frac{\partial u}{\partial x} + v \frac{\partial u}{\partial y} = \nu \frac{\partial^2 u}{\partial y^2} + g\beta(T - T_\infty) - \frac{\sigma^* B_0^2}{\rho} u \quad (2)$$

$$u \frac{\partial T}{\partial x} + v \frac{\partial T}{\partial y} = \alpha \frac{\partial^2 T}{\partial y^2} \quad (3)$$

where  $u$  and  $v$  are the  $x$ (along the plate) and the  $y$ (normal to the plate) components of the velocity respectively;  $g$  is the acceleration due to gravity;  $x, y$  are the Cartesian coordinates,  $B_0$  is the Magnetic field intensity,  $\beta$  is the coefficient of thermal expansion,  $\rho$  is the density of the fluid,  $\nu$  is the Kinematic viscosity,  $\alpha$  is the coefficient of thermal conductivity,  $T$  is the temperature of

the fluid,  $\sigma^*$  is the electrical conductivity and it is variable with temperature as given below

$$\sigma^* = \frac{\sigma}{1+\varepsilon\theta} \quad (4)$$

$\varepsilon$  is the electrical conductivity parameter. All prime symbols denotes differentiation with respect to  $\eta$

The velocity boundary conditions can be expressed as:

$$u(x, 0) = v(x, 0) = 0 \quad (5)$$

$$u(x, \infty) = U_\infty \quad (6)$$

The boundary conditions at the plate surface and far into the cold fluid may be written as:

$$-k \frac{\partial T}{\partial y}(x, 0) = h_f [T_f - T(x, 0)] \quad (7)$$

$$T(x, \infty) = T_\infty \quad (8)$$

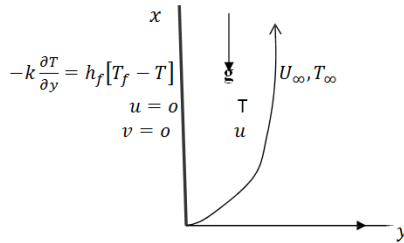


**Fig. 1. Flow Configuration and coordinate system**

Introducing the stream function  $\psi(x,y)$  such that

$$\left. \begin{aligned} u &= \frac{\partial \psi}{\partial y} \\ v &= -\frac{\partial \psi}{\partial x} \end{aligned} \right\} \quad (9)$$

where

$$\Psi = (x, y) = x \sqrt{\frac{U_\infty y}{\nu}} f(\eta), \quad U_\infty = ax \quad (10)$$

The similarity variable  $\eta$ , a dimensionless stream function  $f(\eta)$  and temperature  $\theta(\eta)$  are given as

$$\left. \begin{aligned} \eta &= y \sqrt{\frac{U_\infty}{\nu x}}, \quad u = ax f'(\eta), \quad v = -\sqrt{ax\nu} f(\eta), \\ \theta &= \frac{T - T_\infty}{T_f - T_\infty} \end{aligned} \right\} \quad (11)$$

Thus, the continuity equation (1) is satisfied with  $u$  and  $v$  of equations (11). Using (11),

equations (2) and (3) are transformed into a set of coupled non-linear ordinary differential equation as

$$f'''(\eta) - f'(\eta)^2 + f(\eta) f''(\eta) - \frac{M}{1+\varepsilon\theta} f'(\eta) + Gr \theta(\eta) = 0 \quad (12)$$

$$\theta''(\eta) + Pr f(\eta) \theta'(\eta) = 0 \quad (13)$$

The boundary conditions (5), (6), (7) and (8) reduced to

$$f(0) = f'(0) = 0, \quad f'(\eta) = 1 \quad \text{as } \eta \rightarrow \infty \quad (14)$$

$$\theta'(0) = -Bi [1 - \theta(x, 0)], \quad \theta(\infty) = 0 \quad (15)$$

where  $Gr = \frac{g\beta(T_f - T_\infty)}{ax^2}$  is the dimensionless Grashof number,  $M = \frac{\sigma\beta_0 a^2}{\rho a}$  is the magnetic parameter,  $Pr = \frac{\nu}{\alpha}$  is the prandtl number and  $Bi = -\frac{h}{k} \sqrt{\frac{\nu}{a}}$  is the Biot number.

It is assumed that equations (12) and (13) have a similarity solution where the parameters  $Gr$  and  $Bi$  are defined as constants.

Solving the governing boundary layer equations (12) and (13) with the boundary conditions (14) and (15) numerically using Runge- Kutta fourth order method along with shooting technique and implemented on maple 17. The step size of 0.001 is used to obtain the numerical solution correct to four decimal places as the criterion of the convergence.

### 3. RESULTS AND DISCUSSION

Numerical calculations have been carried out for different values of the thermo physical parameters controlling the fluid dynamics in the flow region.

Table 1 shows the comparison of Makinde's work (2010) with the present work for Prandtl number  $Pr=0.72$  and it is noted that there is a perfect agreement in the absence of Grashof number  $G_r$ . Table 2, illustrates the values of the skin-friction coefficient  $f'(0)$  and the local Nusselt number  $-\theta'(0)$  for various values of embedded parameters. The Graphs below show the Velocity and the Temperature Profiles at various parameter values.

From Table 2 and Figs. 6, 8 and 10, it is observed that the skin-friction and the rate of heat

transfer at the plate surface increases with an increase in local Grashof number  $Gr$ , electrical conductivity parameter  $\varepsilon$  and convective surface heat transfer parameter  $Bi$ . It is also observed that for values of  $Gr > 0$  as in Fig. 7 there is decrease in the temperature profile which corresponds to the cooling problem. The cooling problem is often encountered in engineering applications; for example, in the cooling of electronic components and nuclear reactors.

However, in Fig. 2 and Fig. 4, an increase in the Prandtl number  $Pr$  and magnetic field parameter  $M$  decreases the skin-friction but increases the rate of heat transfer at the plate surface. This is attributed to the fact that as the prandtl number decrease, the thermal boundary layer thickness increases, causing reduction in the temperature gradient  $\theta'(0)$  at the surface of the plate.

In Fig. 3 the temperature gradient reduces at the surface because low prandtl number has high thermal conductivity, causing the fluid to attain higher temperature thereby reducing the heat flux at the surface. Moreover, for such low prandtl number, the velocity boundary layer is inside the thermal boundary layer and its thickness reduces as Prandtl number decreases and so the fluid motion is confined in more and more thinner layer near the surface and thereby experiencing drag increase (skin-friction) by the fluid. In other words there is more straining motion inside velocity boundary layer resulting in the increase of skin-friction coefficient. It is also observed from Table 2 that increase in magnetic field intensity, the skin-friction coefficient decreases the rate of heat transfer near the surface; hence the surface experiences reduction in drag.

**Table 1. Computations showing comparison of the Makinde (2010) and the present result**

| <b>M = Gr = 0 and Pr = 0.72</b> |                                 |                               |                                 |                               |
|---------------------------------|---------------------------------|-------------------------------|---------------------------------|-------------------------------|
| <b>Bi</b>                       | <b>Makinde 2010</b>             |                               | <b>Present Work</b>             |                               |
|                                 | <b><math>-\theta'(0)</math></b> | <b><math>\theta(0)</math></b> | <b><math>-\theta'(0)</math></b> | <b><math>\theta(0)</math></b> |
| 0.05                            | 0.0428                          | 0.1447                        | 0.0428                          | 0.1447                        |
| 0.10                            | 0.0747                          | 0.2528                        | 0.0747                          | 0.2528                        |
| 0.20                            | 0.1139                          | 0.4035                        | 0.1139                          | 0.4035                        |
| 0.40                            | 0.1700                          | 0.5750                        | 0.1700                          | 0.5750                        |
| 0.60                            | 0.1981                          | 0.6699                        | 0.1981                          | 0.6699                        |
| 0.80                            | 0.2159                          | 0.7302                        | 0.2159                          | 0.7302                        |
| 1.00                            | 0.2282                          | 0.7718                        | 0.2282                          | 0.7718                        |
| 5.00                            | 0.2791                          | 0.9442                        | 0.2791                          | 0.9442                        |
| 10.00                           | 0.2871                          | 0.9713                        | 0.2871                          | 0.9713                        |
| 20.00                           | 0.2913                          | 0.9854                        | 0.2913                          | 0.9854                        |

Source: Maple 17 Output

**Table 2. Computational table showing  $f''(0)$ ,  $-\theta'(0)$  and  $\theta(0)$**

| <b>Pr</b>   | <b>M</b>   | <b>Gr</b>  | <b><math>\varepsilon</math></b> | <b>Bi</b>  | <b><math>f''(0)</math></b> | <b><math>-\theta'(0)</math></b> | <b><math>\theta(0)</math></b> |
|-------------|------------|------------|---------------------------------|------------|----------------------------|---------------------------------|-------------------------------|
| <b>0.72</b> | 0.1        | 0.1        | 0.1                             | 0.1        | 0.0780                     | 0.0684                          | 0.3157                        |
| <b>1</b>    | 0.1        | 0.1        | 0.1                             | 0.1        | 0.0739                     | 0.0704                          | 0.2959                        |
| <b>3</b>    | 0.1        | 0.1        | 0.1                             | 0.1        | 0.0613                     | 0.0767                          | 0.2335                        |
| 0.72        | <b>0.1</b> | 0.1        | 0.1                             | 0.1        | 0.0780                     | 0.0684                          | 0.3157                        |
| 0.72        | <b>1</b>   | 0.1        | 0.1                             | 0.1        | 0.0348                     | 0.0602                          | 0.3977                        |
| 0.72        | <b>3</b>   | 0.1        | 0.1                             | 0.1        | 0.0231                     | 0.0574                          | 0.4260                        |
| 0.72        | 0.1        | <b>0.1</b> | 0.1                             | 0.1        | 0.0780                     | 0.0684                          | 0.3157                        |
| 0.72        | 0.1        | <b>1</b>   | 0.1                             | 0.1        | 0.3053                     | 0.0744                          | 0.2565                        |
| 0.72        | 0.1        | <b>3</b>   | 0.1                             | 0.1        | 0.6182                     | 0.0779                          | 0.2207                        |
| 0.72        | 0.1        | 0.1        | <b>0.1</b>                      | 0.1        | 0.0780                     | 0.0684                          | 0.3157                        |
| 0.72        | 0.1        | 0.1        | <b>1</b>                        | 0.1        | 0.0798                     | 0.0686                          | 0.3144                        |
| 0.72        | 0.1        | 0.1        | <b>3</b>                        | 0.1        | 0.0825                     | 0.0688                          | 0.3122                        |
| 0.72        | 0.1        | 0.1        | 0.1                             | <b>0.1</b> | 0.0780                     | 0.0684                          | 0.3157                        |
| 0.72        | 0.1        | 0.1        | 0.1                             | <b>1</b>   | 0.1360                     | 0.1934                          | 0.8066                        |
| 0.72        | 0.1        | 0.1        | 0.1                             | <b>10</b>  | 0.15452                    | 0.2405                          | 0.9760                        |

Source: Maple 17 Output

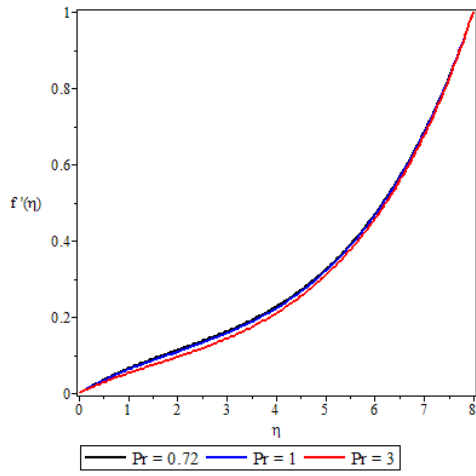


**Fig. 2. Velocity profile for Pr**

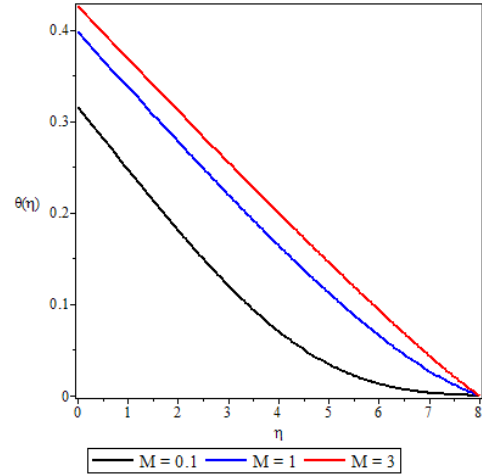


**Fig. 5. Temperature profile for M**

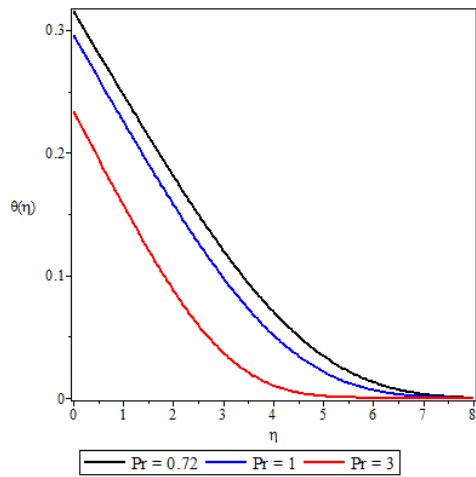


**Fig. 3. Temperature profile for Pr**

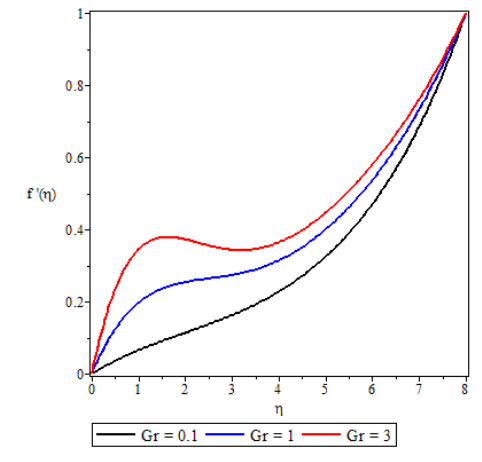


**Fig. 6. Velocity profile for Gr**

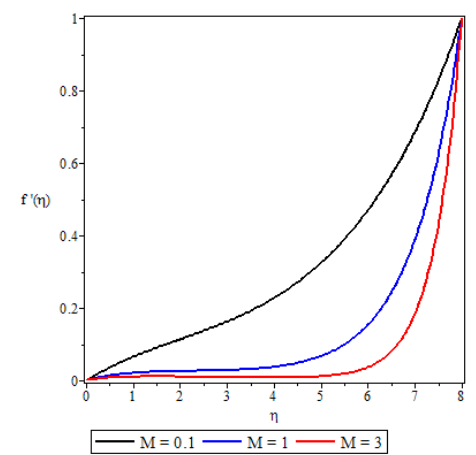


**Fig. 4. Velocity profile for M**

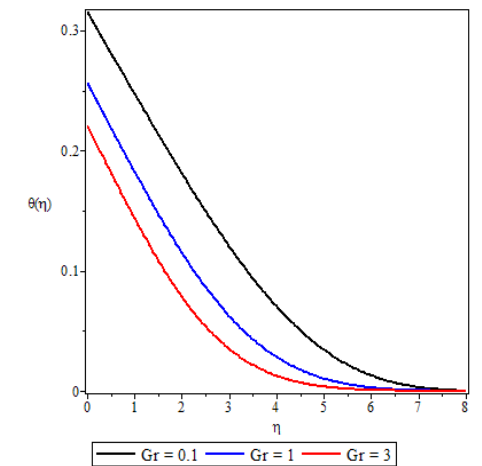


**Fig. 7. Temperature profile for Gr**

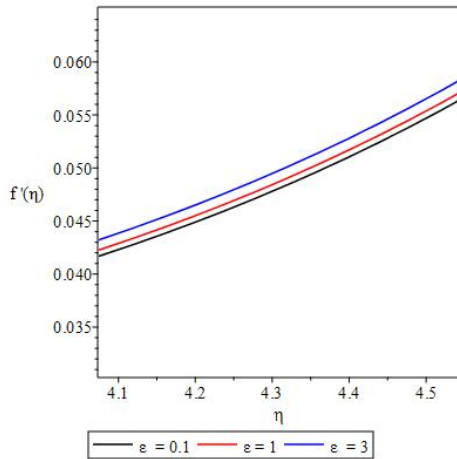


**Fig. 8. Velocity profile for  $\epsilon$**

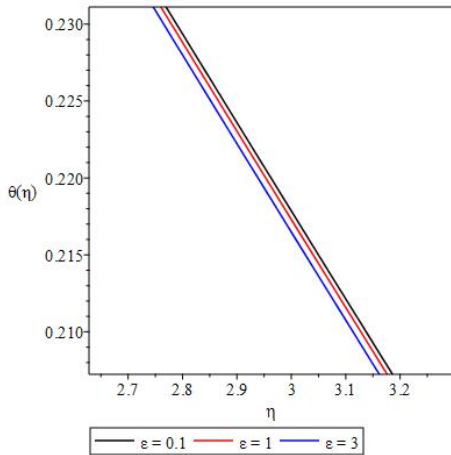


**Fig. 9. Temperature profile for  $\epsilon$**

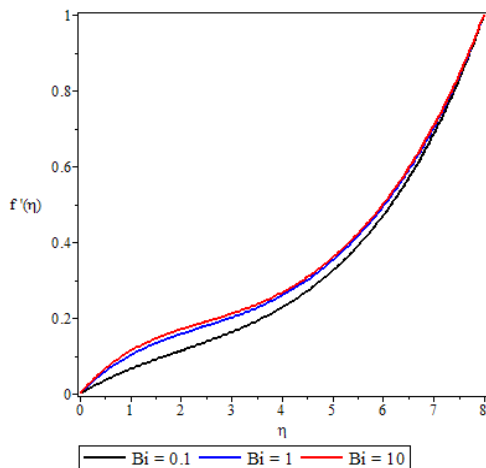


**Fig. 10. Velocity profile for  $B_i$**

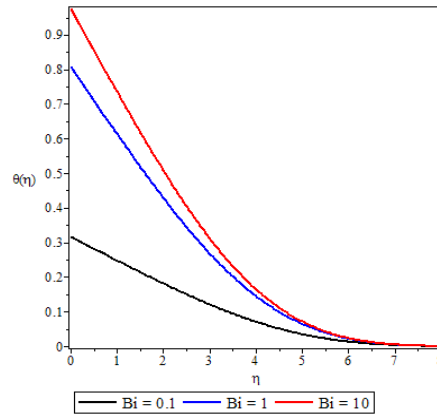


**Fig. 11. Temperature profile for  $B_i$**

Figs. 2, 4, 6, 8 and 10 show that the fluid velocity is zero at the plate surface and increases gradually away from the plate towards the free stream value satisfying the boundary conditions. Also, Figs. 3, 5, 7, 9 and 11 show that the fluid temperature is maximum at the plate surface and decreases exponentially to zero value far away from the plate satisfying the boundary conditions.

#### 4. CONCLUSION

From the numerical solutions and graphical representations, increasing the Prandtl number and the Grashof number tend to reduce the thermal boundary layer thickness. Fluid temperature increases with increase in magnetic field intensity and decreases with increase in electrical conductivity parameter. Fluid velocity increases with increase in electrical conductivity parameter while it decreases with increase in magnetic field intensity.

Thermal boundary layer thickness increases with an increase in biot numbers  $B_i$  and decreases with an increase in Grashof  $Gr$  and Prandtl  $Pr$  numbers. Thus, convective surface heat transfer enhances thermal diffusion while an increase in the prandtl number slows down the rate of thermal diffusion within the boundary layer. Fluid temperature increases due to increase in magnetic field intensity while it decreases due increase or decrease in electrical conductivity parameter.

#### ACKNOWLEDGEMENT

We appreciate the comments of the reviewers in improving the quality of the paper.

## COMPETING INTERESTS

Authors have declared that no competing interests exist.

## REFERENCES

1. Blasius H. Grenzschichten in Flüssigkeiten and Mit Kleiner reibung. Zeitschrift für Angewandte Mathematik und Physik. 1908;56:1-37. French.
2. Aziz A. A similarity solution for laminar thermal boundary layer over a flat plate with a convective surface boundary condition. Communications in Nonlinear Science and Numerical Simulation. 2009; 14:1064–1068.
3. Bataller RC. Radiation effects for the Blasius and Sakiadis flows with a convective surface boundary condition. Journal of Applied Mathematics and Computation. 2008;206:832–840.
4. Cortell R. Numerical solutions of the Classical Blasius flat-plate problem. Applied Mathematics and Computation. 2005;170: 706–710.
5. Cortell R. Similarity solutions for flow and heat transfer of a quiescent fluid over a nonlinearly stretching surface. Journal of Matter Process Technology. 2008;203: 176–183.
6. Gabriella, Bognar. Numerical method for the boundary layer problem of non-Newtonian fluid flow along moving surfaces. Electronic Journal of Qualitative theory of Differential Equations. 2016;122: 1-11.
7. He JH. A simple perturbation approach to Blasius equation. New York Journal of Applied Mathematics and Computation. 2003;140:217–222.
8. Makinde OD, Olanrewaju PO. Buoyancy effects on thermal boundary layer over a vertical plate with convective surface boundary conditions. ASME Journal of Fluids Engineering. 2010;132:231-241.
9. Olanrewaju PO, Arulogun OT, Adebimpe K. Internal heat generation effect on thermal boundary layer with a convective boundary condition. America Journal of Fluid Dynamics. 2012;2(1):1-4.
10. Makinde OD. Analysis of Non-Newtonian reactive flow in a cylindrical pipe. ASME Journal of Applied Mechanics. 2009;76: 034502.
11. Makinde OD, Sibanda P. Magnetohydrodynamic mixed convective flow and heat and mass transfer past a vertical plate in a porous medium with constant wall suction. ASME Journal of Heat Transfer. 2008;130: 112602.
12. Shrama PR, Gurminder S. Steady MHD. Natural convection flow with variable electrical conductivity and heat generation along an isothermal vertical plate. Tamkang Journal of Science and Engineeringvol. 2010;13:235-242.
13. Watunade T, Pop I. Thermal boundary layer in magnetohydrodynamics flow over a flat plate in the presence of a transverse magnetic field. "Acta Mechanica". 1994; 105:233-238.

## APPENDIX

```

> restart
> with(ODETools) :
> with(student) :
> with(plots) :
> with(plottools) :
> inf := 8 :
> equ1 := diff(f(η), η$3) - diff(f(η), η) + f(η) · diff(f(η), η$2) -  $\frac{m}{1 + \epsilon \cdot \theta(\eta)}$ 
    · diff(f(η), η) + Gr · θ(η) = 0

equ1 :=  $\frac{d^3}{d\eta^3} f(\eta) - \left( \frac{d}{d\eta} f(\eta) \right) + f(\eta) \left( \frac{d^2}{d\eta^2} f(\eta) \right) - \frac{m \left( \frac{d}{d\eta} f(\eta) \right)}{1 + \epsilon \theta(\eta)} + Gr \theta(\eta) = 0$ 

> equ2 := diff(θ(η), η$2) + Pr · f(η) · diff(θ(η), η) = 0
equ2 :=  $\frac{d^2}{d\eta^2} \theta(\eta) + Pr f(\eta) \left( \frac{d}{d\eta} \theta(\eta) \right) = 0$ 

> Bi := 0.1 :
> Bcs := f(0) = 0, f'(0) = 0, f'(inf) = 1, θ'(0) = -Bi · (1 - θ(0)), θ(inf) = 0
Bcs := f(0) = 0, D(f)(0) = 0, D(f)(8) = 1, D(θ)(0) = -0.1 + 0.1 θ(0), θ(8) = 0
> Params := [m = 0.1, ε = 0.1, Gr = 0.1, Pr = 0.72] :
> S1 := dsolve({subs(Params, equ1), subs(Params, equ2), Bcs}, {f(η), θ(η)}, type
    = numeric) :
> F1 := odeplot(S1, [ [η, f(η)] ], 0..inf, linestyle = solid, color = black, legend = "m = 0.1",
    labels = ["η", "f(η)"], axes = "boxed") :
> T1 := odeplot(S1, [ [η, θ(η)] ], 0..inf, linestyle = solid, color = black, legend = "m = 0.1",
    labels = ["η", "θ(η)"], axes = "boxed") :
> #####
    #####
> Params := [m = 1, ε = 0.1, Gr = 0.1, Pr = 0.72] :
> S2 := dsolve({subs(Params, equ1), subs(Params, equ2), Bcs}, {f(η), θ(η)}, type
    = numeric) :
> F2 := odeplot(S2, [ [η, f(η)] ], 0..inf, linestyle = solid, color = red, legend = "m = 1", axes
    = "boxed") :
> T2 := odeplot(S2, [ [η, θ(η)] ], 0..inf, linestyle = solid, color = red, legend = "m = 1", axes
    = "boxed") :
> #####
    #####
> Params := [m = 3, ε = 0.1, Gr = 0.1, Pr = 0.72] :
> S3 := dsolve({subs(Params, equ1), subs(Params, equ2), Bcs}, {f(η), θ(η)}, type
    = numeric) :

```



```
> F3 := odeplot(S3, [ [η, f(η) ]], 0..inf, linestyle = solid, color = blue, legend = "m = 3", axes  
= "boxed") :  
> T3 := odeplot(S3, [ [η, θ(η) ]], 0..inf, linestyle = solid, color = blue, legend = "m = 3", axes  
= "boxed") :  
>  
> plots[display](F1, F2, F3); plots[display](T1, T2, T3);
```

---

© 2018 Fenuga et al.; This is an Open Access article distributed under the terms of the Creative Commons Attribution License (<http://creativecommons.org/licenses/by/4.0>), which permits unrestricted use, distribution, and reproduction in any medium, provided the original work is properly cited.

*Peer-review history:*  
*The peer review history for this paper can be accessed here:*  
<http://www.sciencedomain.org/review-history/23124>